DOT/FAA/PM-87/6

Program Engineering
and Maintenance Service
Washington, D.C. 20591

Low-Altitude Wind Shear Detection With Doppler Radar

Michael D. Eilts

National Severe Storms Laboratory
1313 Halley Circle
Norman, OK 73096

February 1987

Final Report

U.S. Department of Transportation
Federal Aviation Administration

NOTICE

This document is disseminated under the sponsorship of the Department of Transportation in the interest of information exchange. The United States Government assumes no liability for its content or use thereof.

Technical Report Documentation Page

1. Report No.	2. Government Accession No.	3. Recipient's Catalog No.
DOT/FAA/PM-87/6	AD-A181 900	

4. Title and Subtitle	5. Report Date
Low Altitude Wind Shear Detection With Doppler Radar	February 1987
	6. Performing Organization Code: MGG000
	8. Performing Organization Report No.

7. Author(s)	
Michael D. Eilts	

9. Performing Organization Name and Address	10. Work Unit No. (TRAIS)
National Severe Storms Laboratory 1313 Halley Circle Norman, OK 73069	11. Contract or Grant No.: DTFA01-80-Y-10524
	13. Type of Report and Period Covered: Final Report

12. Sponsoring Agency Name and Address	14. Sponsoring Agency Code
U.S. Department of Transportation Federal Aviation Administration Program Engineering and Maintenance Service Washington, D.C. 20591	APM-310

15. Supplementary Notes

16. Abstract The feasibility of using the next generation weather radar (NEXRAD) system to detect low-altitude horizontal wind shear near airports is investigated. We compare surface-measured horizontal shear with that observed aloft with Doppler radar to determine how the radar-estimated shear above the surface relates to the surface-measured shear. For five Oklahoma gust fronts, the Doppler radar estimate of shear (at heights between 50-600 m) averaged 1.6 times the shear measured at the surface. For none of 43 comparisons was the surface radial velocity difference across the gust front stronger than the radial velocity difference measured by Doppler radar aloft. When the five gust fronts passed an instrumented tower a vertical profile through the lowest 440 m of the gust front could be determined. In all cases the wind speed and wind shear increased in the lowest 90 m of the atmosphere. In one case, the 90 m height had the peak wind shear; in all other cases the peak wind shear was at a much higher altitude. The Federal Aviation Administration requires that NEXRAD radar coverage have a lowest scan of 60 m above the surface in the airport area (within 20 km of the airport); the strongest shears in the five gust fronts investigated in this study were at the 90 m or higher levels of the tower. Due to surface friction it is expected that wind speeds and shears in downbursts will also be stronger aloft than at the surface, however, further study is necessary. It is suggested that a combination of Doppler radar data and information gleaned from a Low-Level Wind Shear Alert System (LLWSAS) would allow more accurate wind shear estimates in the terminal area of airports than would be possible with either system by itself.

17. Key Words	18. Distribution Statement
wind shear; Doppler radar; gust fronts	This document is available to the public through the National Technical Information Service, Springfield, Virginia 22161.

19. Security Classif. (of this report)	20. Security Classif. (of this page)	21. No. of Pages	22. Price
UNCLASSIFIED	UNCLASSIFIED	38	

Form DOT F 1700.7 (8-72) Reproduction of completed page authorized

Preface

The author would like to thank Dr. Richard Doviak for the benefit of our many discussions. I also thank my colleagues at the National Severe Storms Laboratory for support and for the data sets on which this study was based. Joan Kimpel and Robert Goldsmith performed graphic services.

TABLE OF CONTENTS

LIST OF FIGURES

LIST OF TABLES

1. Introduction

The capabilities and limitations of Doppler radar to detect horizontal wind shear hazards to flight at near-surface altitudes which are below the radar beam axis has been investigated. It is unreasonable to expect that a Doppler radar, sited near an airport, will be able to directly measure winds in the lowest 50 m above the surface due to ground clutter, beam blockage, and the height of the radar horizon. Thus it is important to ascertain what the relationship is between the shears near the surface and the shears measured by Doppler radar aloft. In this study it is assumed that measurement of winds with Doppler radar at an altitude of approximately 60 m above the surface in the airport area, will be possible, which is the lowest altitude coverage requirement for the proposed NEXRAD radars set by the FAA (1981). Other considerations for the measurement of low-altitude wind shear with Doppler radar related to the characteristics of the wind shear phenomena, such as the asymmetry of outflows, lifetimes, etc., are not in the scope of this paper and have been previously, and are still being studied (e.g., Eilts and Doviak, 1986; Wilson et al., 1984; and Mahapatra et al., 1983).

Although numerous processes can cause low-altitude wind shear, downdrafts from convective storms cause some of the most severe shears. Low-altitude wind shear associated with thunderstorms has been implicated in a number of aircraft accidents (National Research Council, 1983). The next generation weather radar system (NEXRAD), which is being developed under a joint program by the Federal Aviation Administration (FAA), the National Weather Service (NWS), and the U. S. Air Force Air Weather Service (AWS), could be used to detect low-altitude shear in the terminal area of airports (Mahapatra and Lee, 1984).

The FAA (1981) identified the following three regions of airspace near airports, each region having different requirements for NEXRAD coverage: 1) the airport area, within 20 km of the airport; 2) the terminal area, 20-56 km from the airport; and 3) the enroute area, >56 km from the airport. Figure 1 shows the FAA requirements for coverage by NEXRAD in these three areas. The lowest altitude coverage requirement is 61 m in the airport area and 150 m in the terminal area. The purpose of this study is to determine if low-elevation angle scans that meet these requirements (or even scans that do not) will be able to detect and estimate wind shear along the ~3° glide slope of landing and departing aircraft, as well as at the surface, even though these heights may be below the radar beam axis.

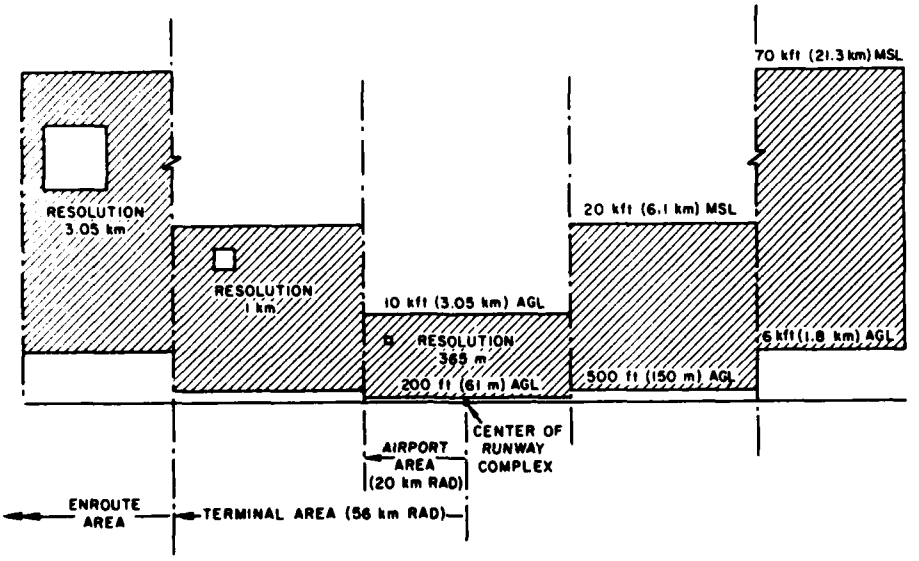

Figure 1. FAA requirements of altitude limits of NEXRAD coverage and resolution in different flight areas.

2. Previous studies

Few quantitative comparisons have been made between Doppler-radar-observed winds and surface-observed winds, especially in regions of horizontal wind shear. Zrnic' and Lee (1983) compared shear estimated by Doppler radar in gust fronts with that measured at the surface by the National Severe Storms Laboratory's (NSSL) SAM (Stationary Automated Mesonetwork) stations. Although no attempt was made to correlate comparisons in time or location, horizontal shears through individual gust fronts were compared. Shear observed at the surface was considerably less than that observed at heights between 100 and 1000 m. The average shear observed by Doppler radar for six gust fronts was five times that observed by surface stations; values ranged from 2.4 to 8.3.

Studies of low-altitude winds caused by microbursts during JAWS indicated that divergence seen in multiple Doppler analyses at low altitudes correlated well with the location of divergence measured on the ground (Hjelmfelt, 1984). Comparisons of anemometer winds (1 min averages) at 3 m height with Doppler-derived low-altitude winds at 20-100 m height for three JAWS microbursts showed that the anemometer winds are typically smaller (Kessinger et al., 1983). Surface winds averaged ~50% lower for one of the microbursts, 60% for another, and only 10% lower for a third case in which the Doppler analysis was at a very low height (i.e., ≈ 10-100 m). This reduction of winds at the surface was attributed to slowing of the winds by frictional forces.

Boundary layer meteorologists have done a number of comprehensive studies on wind profiles in the planetary boundary layer. One such study (Clarke, 1970) showed that for all types of atmospheric stability, wind speed increased on the average from the surface up to heights of ~400 m. The strongest change of wind speed with height is in the surface layer -- the lowest 5 to 100 m of the boundary layer.

The change of wind in the vertical in the surface layer can be expressed by (Businger et al., 1971)

$$\frac{\partial \bar{u}}{\partial z} = \frac{u_*}{kz}(1-15\zeta)^{-1/4} \text{ for } \zeta < 0 \quad \text{(unstable)} \tag{1}$$

$$\frac{\partial \bar{u}}{\partial z} = \frac{u_*}{kz}(1+4.7\zeta) \text{ for } \zeta > 0 \quad \text{(stable)} \tag{2}$$

where $\bar{u}$ is the magnitude of the mean horizontal wind vector, z is the height, u_* is the friction velocity, k is the von Karman constant, and $\zeta = z/L$ is a nondimensional height where L is the Obukhov length which is negative in unstable conditions and positive in stable conditions. From (1) and (2) we can see that $d\bar{u}/dz$ is always positive in the surface layer. Thus the mean winds increase with height in all stability conditions. For neutral conditions ($\zeta = 0$) the wind speed logarithmically increases with height:

$$u(z) = \frac{u_*}{k} \ln z/z_o$$

where z_o is the roughness length.

Although (1) - (3) were determined using data collected in a fairly steady state and undisturbed environment and not in convective storms, a similar increase of winds in the lowest 50-100 m of the atmosphere has been observed within thunderstorm outflows (see, e.g., Klingle, 1985; Bedard et al., 1979; Goff et al., 1977; Wilson et al., 1984).

Because of this increase of wind speed with height both in the nonstormy air and within thunderstorm outflows, it is proposed that shears also will be weaker near the surface than aloft.

To show how the logarithmic profile is responsible for shears aloft being

stronger than shears at the surface, we will make some simplifying assumptions: (1) Flow in the atmosphere is perpendicular to the shear zone so that winds ahead and behind the shear zone are parallel but opposite in direction. (2) Wind is unidirectional with height. (3) In the surface layer, stability is neutral on both sides of the shear zone. (4) u_* and z_0 are constants. The value of z_0 = 0.1 m was used in accordance with Eilts (1983), who computed this value for the area around the KTVY instrumented tower located near Oklahoma City. With these assumptions we can use equation (3) to determine wind speed at different heights within the surface layer. Figure 2 schematically shows this simplified shear zone for both convergent and divergent shear along with the wind profiles on either side. Of course, the logarithmic profile does not always extend to large heights above the surface but evidence from the published literature seem to support winds increasing with height up to at least 50 m above ground level in thunderstorm outflows as well as within the surrounding convective boundary layer. An estimation of the ratio of shear aloft (say, 90 m) to shear at the height of the surface measurements (6 m) using the assumptions listed above, yields a ratio of 1.7:1. This ratio is dependent on the value of z_0 which suggests that this ratio will be larger with increased surface roughness. Above the surface layer we expect that winds will remain fairly constant with height in the convective boundary layer (Kaimal et al., 1976). If this also holds true for storm outflows, we would expect horizontal shear to remain fairly constant above the surface layer up to the top of the outflow phenomena (e.g., a few hundred m for microbursts and up to 1 km or more in gust fronts).

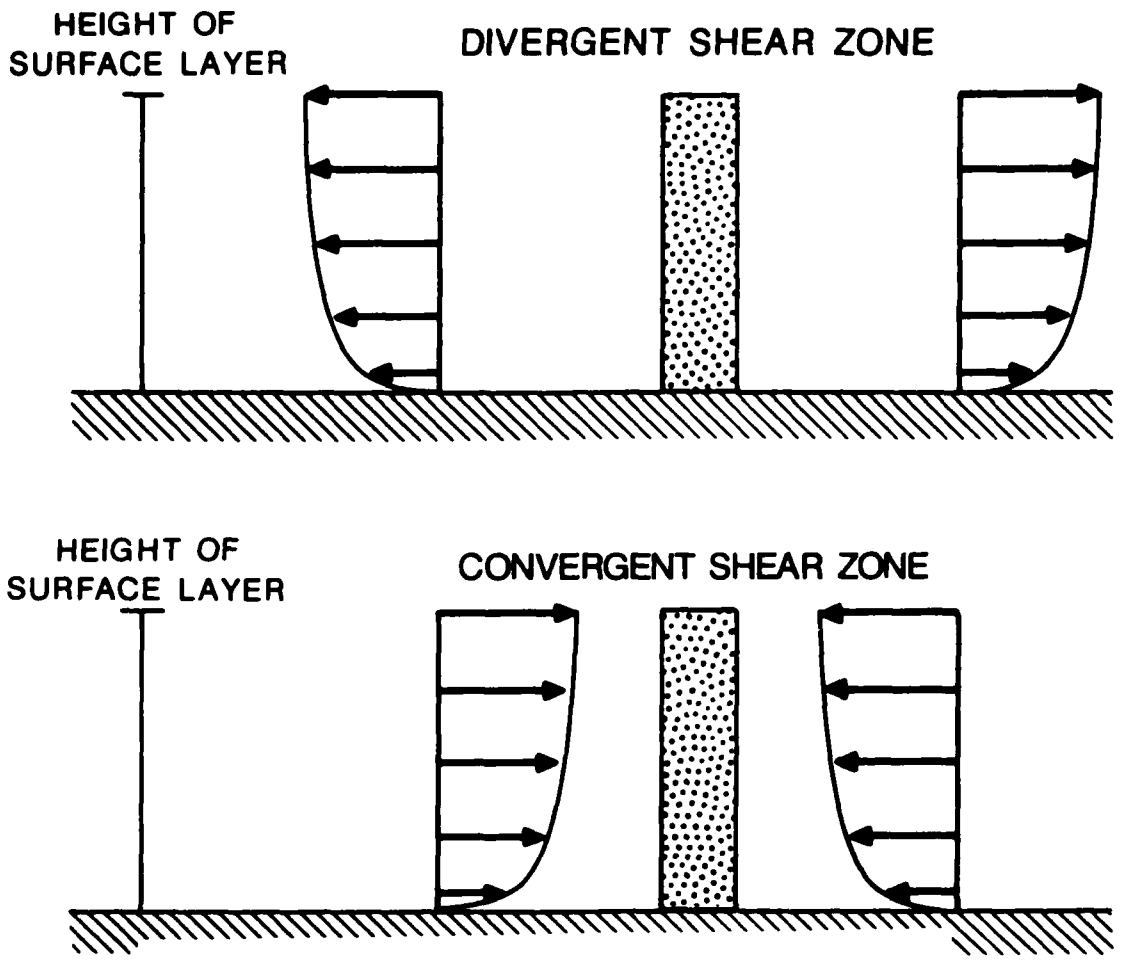

Figure 2. Convergent and divergent shear zones showing wind profiles on either side. Note that the strongest shears are at the top of the surface layer.

3. Data

In order to determine the relationship between horizontal wind shear observed by Doppler radar and that measured near the surface, it is desirable to have a large number of points for comparison. In the Oklahoma environment, gust fronts often cause some of the strongest shears at low altitudes. Gust fronts have been studied by a number of investigators (e.g., Goff et al., 1977; Zrnic' and Lee, 1983; Wakimoto, 1982; and Klingle, 1985). A gust front

is the leading edge of the horizontally propagating outflow from a thunderstorm. Because gust fronts are long-lived phenomena that move quite rapidly and have fairly large horizontal dimensions, they are ideal for a study like this.

The National Severe Storms Laboratory (NSSL) operates a 450 m instrumented tower, two Doppler radars, and a number of SAM stations each spring (Fig. 3). Data from these sensors were used for a comparison of low-altitude horizontal shears caused by gust fronts.

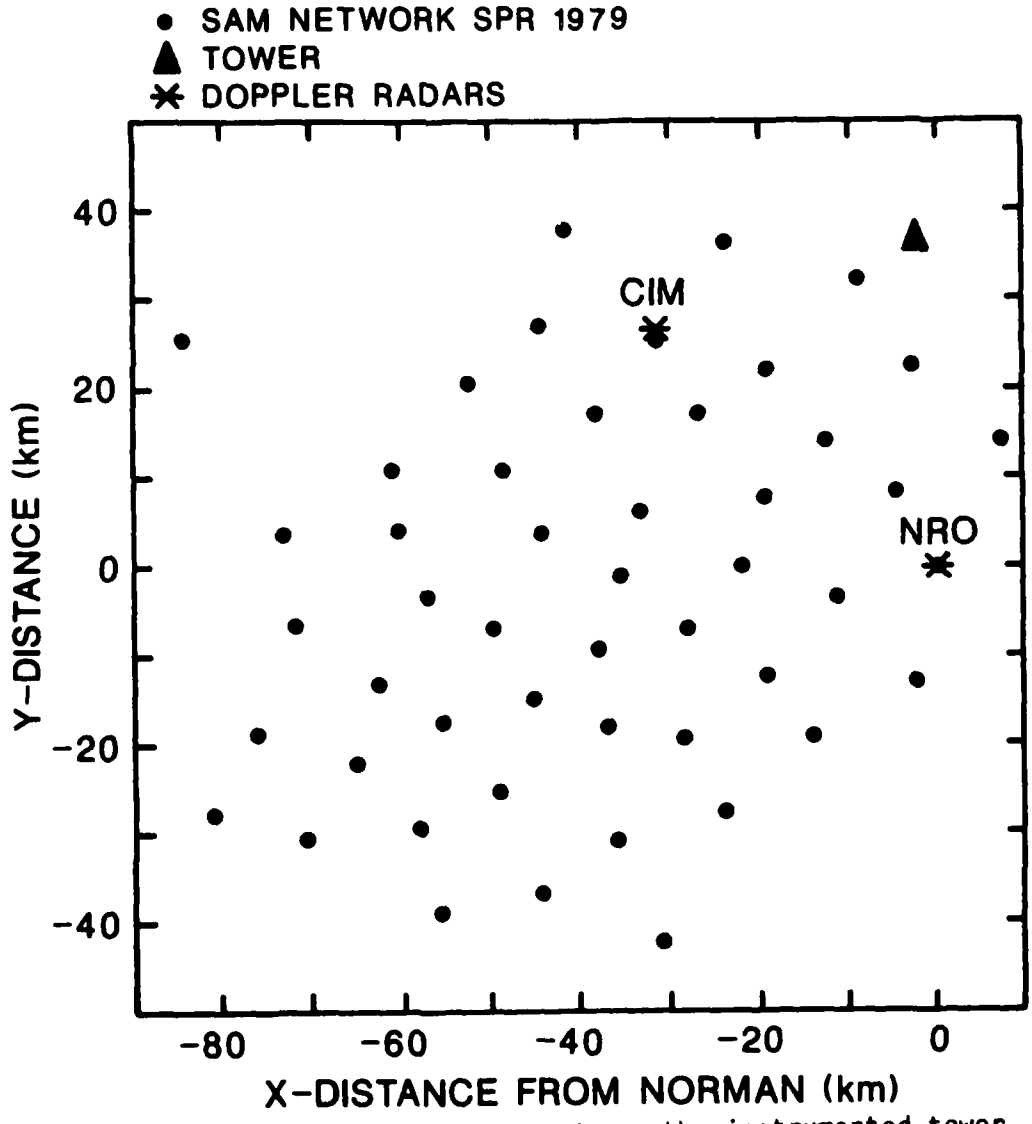

Figure 3. Location of the two Doppler radars, the instrumented tower, and the 1979 SAM stations.

Cases were selected so that at least one Doppler radar was viewing the gust front at a nearly perpendicular angle when the gust front was passing over a SAM station. The years 1979 and 1984 afforded the best opportunities for comparison since a large number of SAM stations were operated in those years. Project SESAME (Severe Environmental Storms and Mesoscale Experiment) operations occurred in central Oklahoma in 1979. As part of this project, 52 SAM stations were set up in a dense network, mainly to the south and west of the two Doppler radars. In 1984, 28 SAM stations were operated, mainly to the south and west. For this reason, two of the stronger gust fronts from 1979 and two from 1984 were selected for study. One other strong gust front that occurred on 30 May 1982 when there was a network of 11 stations was also chosen.

4. The Cases

1) May 2, 1979

On May 2, 1979 two gust fronts passed through the surface mesonetwork. Figure 4 shows the surface network winds at 2110 CST when two gust fronts were in the area. The one which runs east-west is an older front that pushed into the mesonet from the NNW at ~2015 CST and by 2110 was nearly stationary. The second gust front was moving from ~300°/13.5 m s^{-1}. Figure 5 is a radial velocity contour (every 5 m s^{-1}) plot at 2110 CST from the Norman radar showing a portion of the gust fronts to the north and west. Unfortunately, the radar beam only scanned as far south at 270°, so no comparisons were possible with over half the stations on this day.

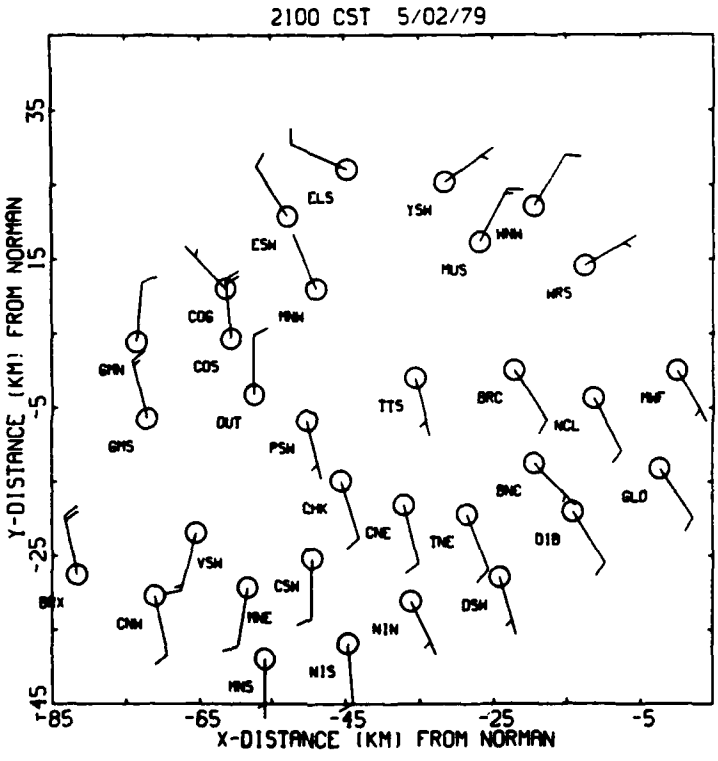

Figure 4. Plot of surface network winds at 2100 CST, May 2, 1979. A full wind barb indicates winds of 5 m s^{-1}.

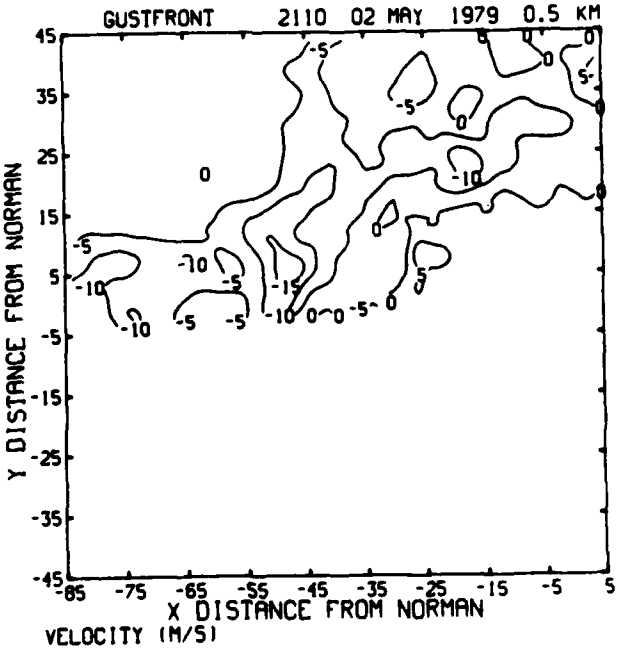

Figure 5. Radial velocity plot from the Norman Doppler radar at 2110 CST, May 2, 1979.

2) June 6, 1979

On June 6, 1979 two gust fronts which eventually merged were observed to the west and south of Norman. The first of the gust fronts was observed directly west of Norman and moved from 270° at 13 m s^{-1}. Figure 6 is the surface wind field as observed by the SAM stations at 1630 CST. Notice the line of divergence behind the gust front where winds are actually out of the S-SE at stations BRX, GMS, COS, ESW, and COG. Figure 7 is the radial velocity contour (every 5 m s^{-1}) plot at the same approximate time (1632 CST) from the Norman Doppler radar. This case was ideal for comparison since the gust front was oriented perpendicular to the radar beam and moved nearly directly towards the Norman radar over a number of surface stations. Another gust front of approximately the same strength also occurred at this time to the southwest of this one. The second gust front was moving to the NNE and eventually the two gust fronts merged to form a single gust front which afforded more shear comparisons with some of the southern most stations.

3) May 30, 1982

As was stated earlier, in 1982 very few SAM stations were operated during the spring program. On May 30 only 11 stations were operational. On this day, a very strong gust front approached central Oklahoma from the west. Figure 8 is the radial velocity plot from the Norman radar at 2056 CST. Figure 9 is the surface plot from the SAM stations at the same time. Radial velocity estimates at 2047 CST from the Norman Doppler radar were as large as 45 m s^{-1} at a height of 400 m. This was one of the strongest gust fronts observed in recent years. From the radial velocity field it appears that there is a secondary surge behind the gust front; this is where the largest velocities were measured. During this time both radars were scanning the gust front and this allowed for good comparison for a number of sites.

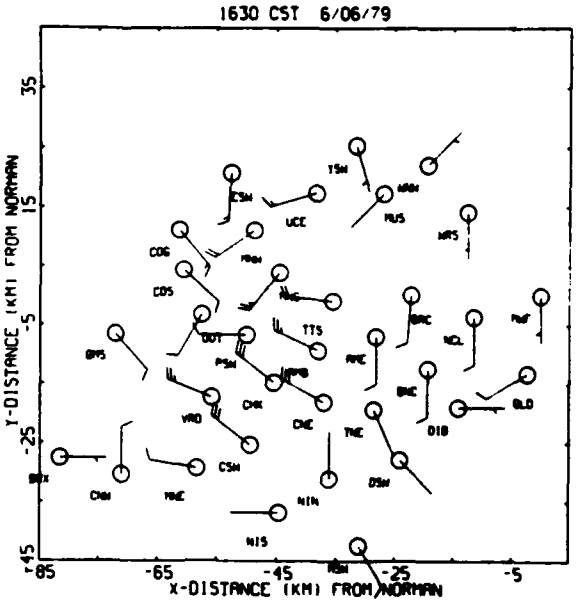

Figure 6. Plot of surface network winds at 1630 CST, June 6, 1979.

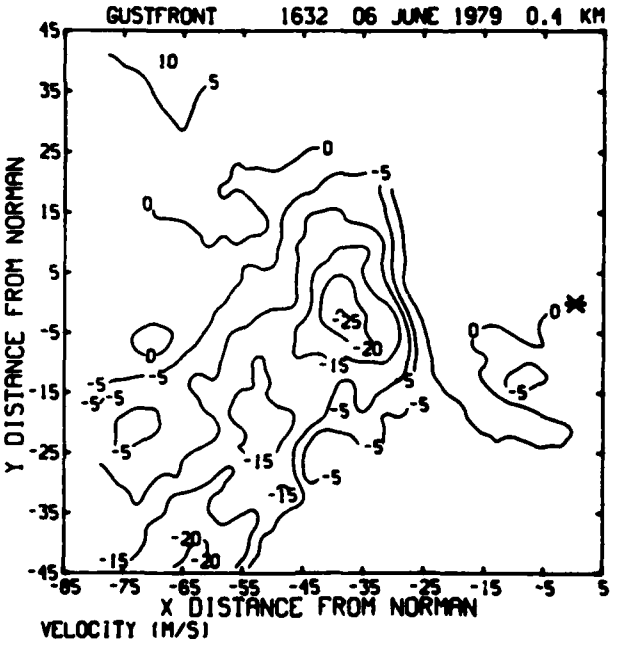

Figure 7. Radial velocity (contoured every 5 m s^{-1}) from the Norman Doppler radar at 1632 CST, June 6, 1979.

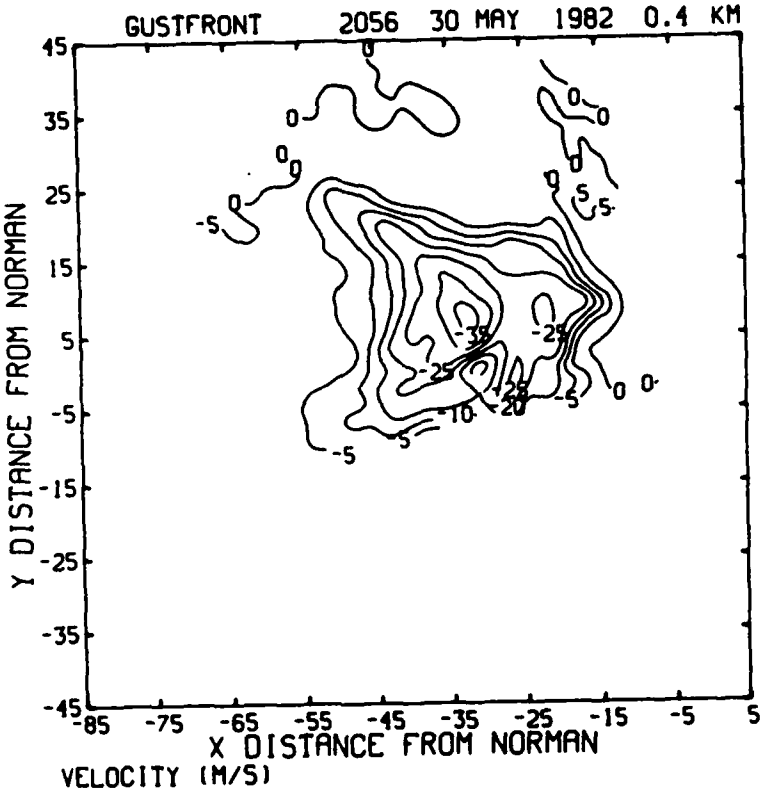

Figure 8. Radial velocity plot (contoured every 5 m s^{-1}) from the Norman Doppler radar at 2056 CST, May 30, 1982.

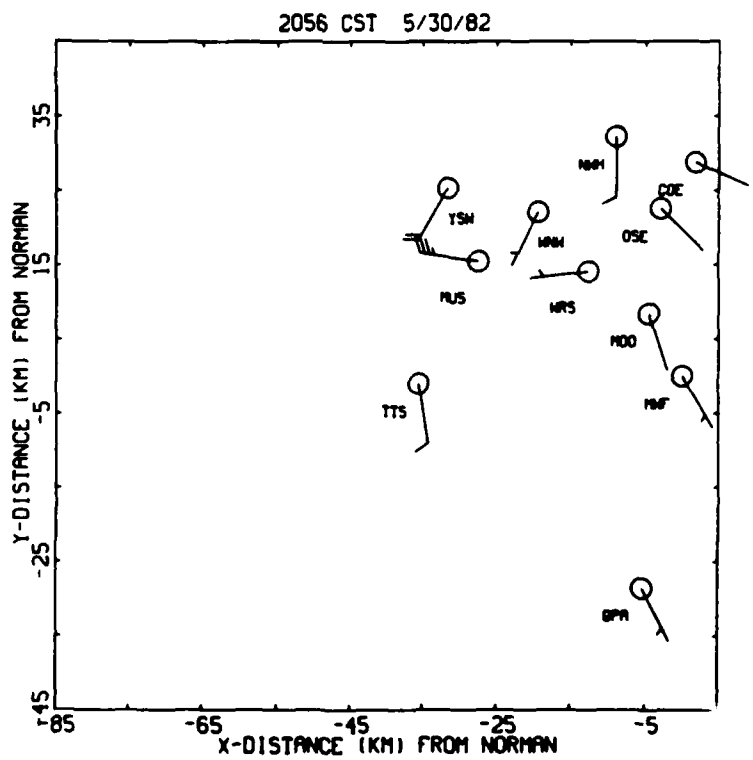

Figure 9. Plot of surface network winds at 2056 CST, May 30, 1982.

4) April 26, 1984

On April 26, 1984 another strong gust front approached Norman from the Northwest. This was a peculiar case because the ambient winds at the surface ahead of the gust front were from the south at 15 m s^{-1} with gusts to 22 m s^{-1} while behind the front winds were out of the WNW at only ~10 m s^{-1} with gusts to 18 m s^{-1}. Yet the gust front propagated to the southeast at ~12 m s^{-1}. A radial velocity plot of this gust front from the Norman Doppler radar at 2047 CST is shown in Fig. 10. The surface wind field at the same time is shown in Fig. 11. This case allowed comparison at a number of sites as the gust front moved through the surface network.

5) May 27, 1984

On May 27, 1984 a long line of thunderstorms ran from northeast Oklahoma to the WSW into the Texas Panhandle (Fig. 12). From this line of thunderstorms a number of reports of straight line wind damage were given (NOAA, 1984). In central Oklahoma, one downburst was observed by the two NSSL radars ~50 km to the NE of Norman at 1630 CST (Eilts and Doviak, 1986). A weak gust front first entered the surface mesonet area at approximately 1515 CST. This gust front slowly moved from the north at approximately 8 m s^{-1}. At this time the Norman Doppler radar was scanning in this direction. However, because the gust front was well out in front of any precipitation, returns were weak and ground clutter contamination rendered the Doppler data useless for comparison purposes. As the gust front moved into the center of the surface mesonet, the gust front remained oriented east-west (Fig. 13) which is parallel to the radar beam, thus very little shear was observed by the Norman radar allowing

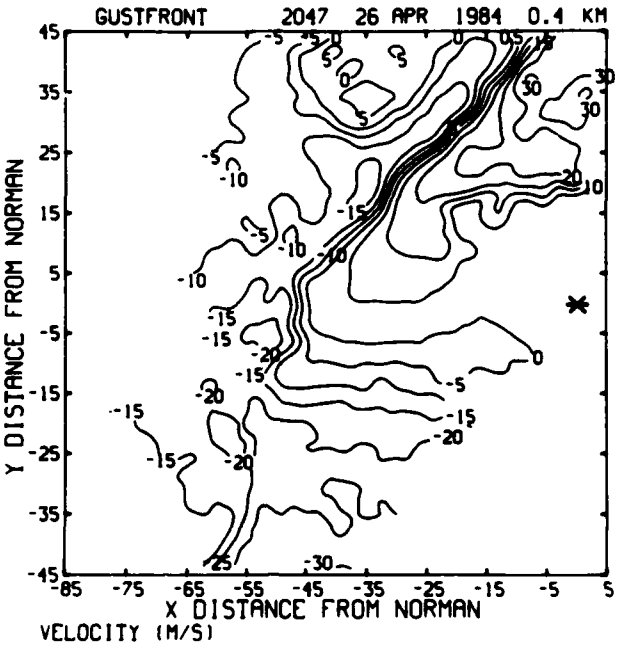

Figure 10. Radial velocity plot (contoured every 5 m s^{-1}) from the Norman Doppler radar at 2047 CST, April 26, 1984.

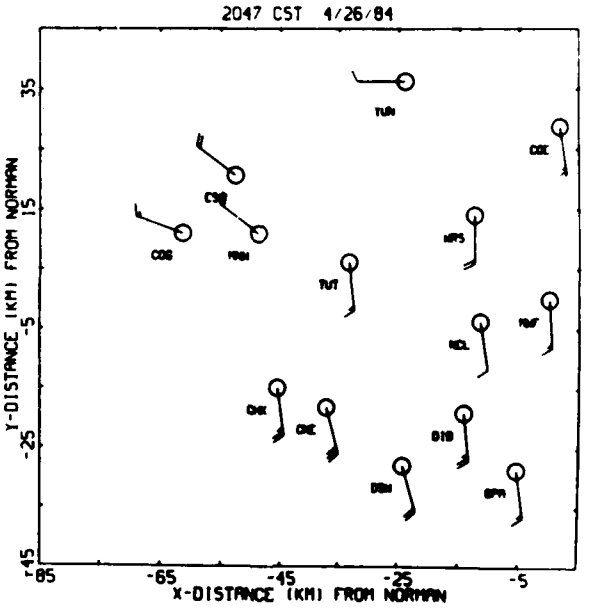

Figure 11. Plot of surface network winds at 2047 CST, April 26, 1984.

no comparison. At 1700 CST the Norman Doppler went into a vertical pointing mode for another experiment and as a result almost no shear comparisons were possible with the Norman radar. The Cimarron radar had similar difficulties, however, four shear comparisons were still possible on this day.

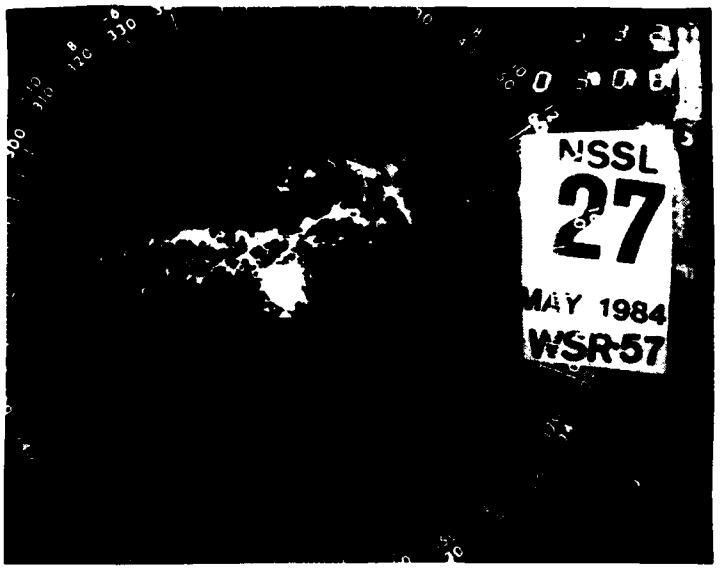

Figure 12. WSR-57 radar at 1632 CST, May 27, 1984 showing line of thunderstorms to the north.

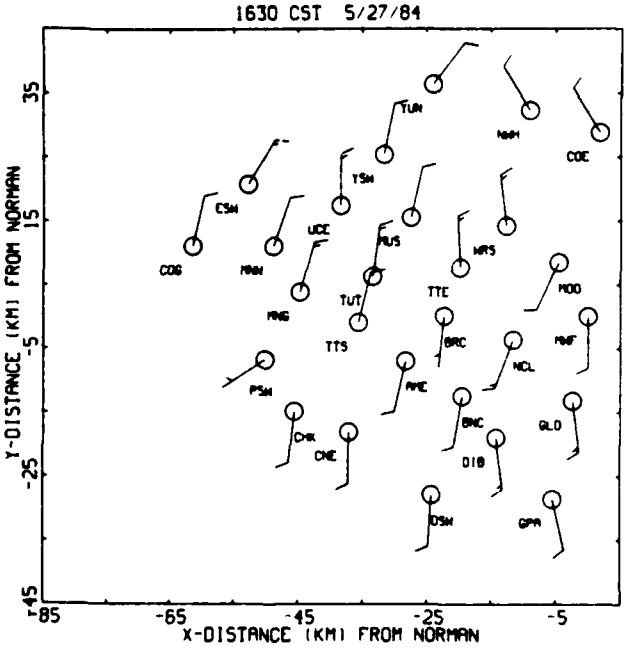

Figure 13. Plot of surface network winds at 1630 CST, May 27, 1984.

5. Data analysis

For shear comparisons, a large number of Doppler radar datasets had to be analyzed. One of the most time-consuming steps in analyzing Doppler radar data is editing and dealiasing the radial velocities. In this study the radial velocity data were edited and dealiased using a local environmental check algorithm (Eilts and Doviak, 1987). The algorithm compares the velocity value in question with nine neighboring points in the same and in the preceding adjacent radial. If the velocity value is not within a band determined by statistical properties of the nine neighboring points, an attempt is made to dealias it into this band; if this cannot be done the velocity value is removed.

After the radial velocity data were edited and dealiased, they were interpolated to a horizontal grid using a Cressman weight (Cressman, 1959) with horizontal radius of influence of 300-750 m depending on the distance from the radar to the grid. No vertical interpolation was necessary because only the lowest elevation angle scan data were used (θ_e = 0.0° - 0.5°).

SAM winds are averaged during data collection over 1 min time. From these data the radial velocity toward or away from the radar was computed for each minute. Tower winds are sampled every 10 s during data collection. The tower data were averaged over a 1 min time interval and the radial velocity toward or away from the radar was computed for each minute.

In order to compare SAM or tower data with the radar data, some time-to-space (or space-to-time) conversion had to be made. This was done by first determining the direction and speed of each gust front. This task was difficult in some cases, especially for days in which the gust front moved at different speeds and direction along its length. Great care was taken in these cases to determine gust front movement at the station location. This was done

by visually inspecting analyzed data from two or more scans of the radar (usually ~5 min apart). From two consecutive scans it was then possible to determine, with some degree of accuracy, the gust front motion.

Once the gust front motion was determined, a set of grid points was established on both sides of the station location with spacing the equivalent of 1 min apart and orientation parallel to the direction of motion (Fig. 14). Then the Doppler radar data were weighted to each grid point using a bi-linear interpolation technique (Gandin, 1965).

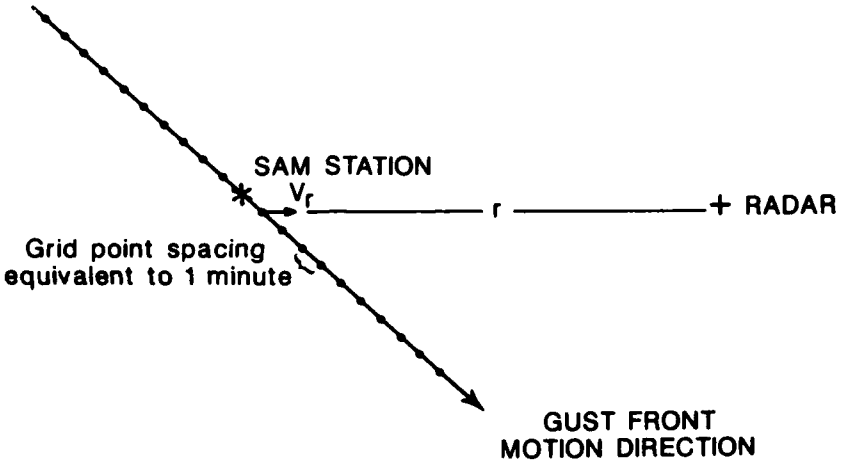

Figure 14. Schematic showing technique used to compare radar radial velocity data with SAM data. In order to make comparison, the SAM wind speed and direction were converted to radial velocity.

This space-to-time conversion was done for a maximum of 10 min (~6 km) on each side of the station location. This assumes that the gust front does not significantly change over the 10 min period (Taylor hypothesis), an assumption supported by comparison of Doppler radar scans as much as 20 min apart in which the gust front is easily identifiable and looks very similar at both times.

For comparison purposes the gust front is taken as the time (SAM data) or distance (radar data) required for the radial velocity to start to decrease (increase) from a usually fairly steady state, and then reach its minimum (maximum) radial velocity. In most cases the gust front passage lasted approximately 10 min. An example of a gust front as determined by the radial velocities from both a SAM site and the Norman Doppler radar is shown in Fig. 15.

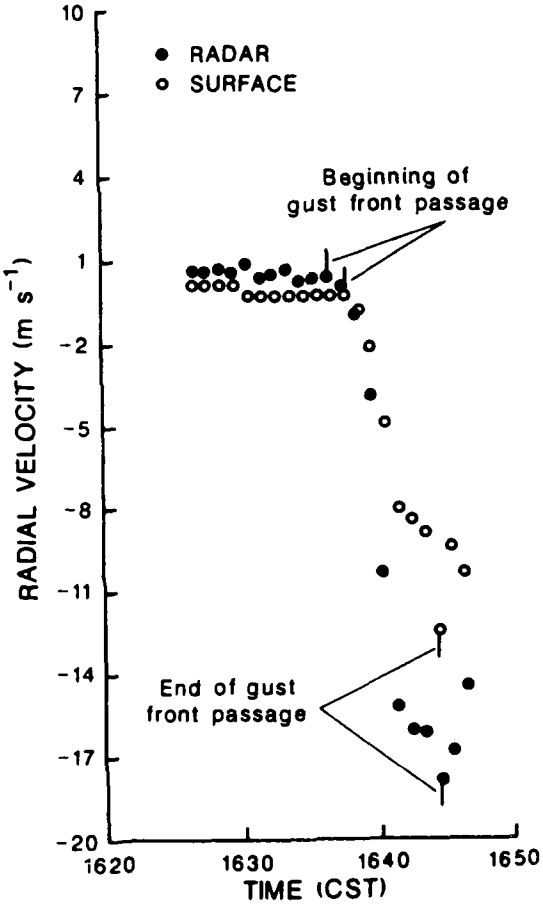

Figure 15. Radial velocity data that have been interpolated to grid points at SAM station BRC along direction of gust front motion from the Norman Doppler radar are compared with calculated radial velocities from the BRC site. The vertical lines in the figure denote beginning and ending of the gust front as determined for comparison purposes.

Individual station comparisons were selected by inspecting the SAM surface velocity data that had been converted to radial velocities toward both Doppler radars. From these radial velocity data, possible comparisons were selected. If either Doppler radar had scanned over the station location at low elevation angle ($\leq 0.5°$) within 5 min of the gust front passage, data from that Doppler radar were analyzed. Several of these Doppler radar analyses proved to be useless for comparison purposes because of ground clutter contamination, gust fronts in the clear air at ranges too far for accurate velocity estimates, or overlaid echoes (Doviak and Zrnic', 1984). Comparisons were used only if the gust front motion could be accurately determined and both the leading and trailing edges of the gust front were within 10 min (~6 km) of the station location. Although it is believed that the accuracy of the gust front motion is good, we have chosen to compare radial velocity differences across the gust front rather than radial shears because radial shear is dependent upon the estimated speed of the gust front, and would only introduce another source of error into the comparison.

6. Results

Figure 16 is a plot of the radial velocity differences across a gust front observed by the radar versus the radial velocity differences observed by the SAM sites. A least-squares fit line drawn through these points has a slope of 1.6, denoting that the radial velocity difference observed aloft by radar on the average is 1.6 times the radial velocity difference observed at the surface. The ratio of 1.6 appears to be independent of the height of the radar beam. Table 1 lists all the comparisons with both their estimated radial velocity difference and radial shear.

Table 1: Surface-measured and radar-measured shear and velocity difference across gust fronts. The distance is the width of the gust front.

		RADAR			SURFACE		
Date	Sta.	Vel. Diff.	Distance	Shear	Vel. Diff.	Distance	Shear
4/26/84	YUN	33 m s^{-1}	6.7 km	$4.9 \times 10^{-3} s^{-1}$	17 m s^{-1}	5.3 km	$3.2 \times 10^{-3} s^{-1}$
	ESW	26	5.3	5.0	20	3.8	5.3
	COG	17	6.0	2.8	12	4.5	2.7
	TUT	21	4.5	4.7	15	5.3	2.9
	MNW	23	5.3	4.4	13	4.5	2.9
5/27/84	WRS	21	2.9	7.3	9	3.8	2.3
	COE	22	1.9	11.5	20	1.9	10.4
	COE	20	10.9	1.8	14	5.5	2.5
	MWF	22	7.2	3.1	15	10.0	1.5
5/30/82	WRS	15	7.2	2.0	13	8.4	1.5
	MUS	27	7.2	3.8	17	8.4	2.0
	TTS	22	3.6	6.0	14	3.6	3.9
	WRS	29	3.6	8.1	14	3.6	3.9
	MWF	23	3.6	6.4	14	4.8	2.8
	MOO	35	8.4	4.1	18	8.4	2.1
	WNW	17	6.0	2.8	10	4.8	2.0
	OSE	20	4.8	4.2	10	3.6	2.8
6/6/79	GMS	21	5.6	3.8	15	7.1	2.1
	VWS	9	3.2	2.8	5	4.8	1.0
	UCE	12	4.8	2.5	9	5.6	1.5
	BRC	18	5.6	3.2	12	5.6	2.2
	MUS	12	5.6	2.2	6	5.6	1.1
	AMB	17	4.8	3.6	13	3.2	4.1
	CNE	18	7.9	2.3	14	7.9	1.8
	TTS	26	11.1	2.3	16	7.9	2.0
	AME	20	5.6	3.6	13	3.2	1.1
	MNG	21	7.1	2.9	12	11.1	1.1
	PSW	23	11.9	1.9	16	9.5	1.7
	BRX	15	4.8	3.1	8	6.4	1.3
	CNW	29	7.9	3.7	16	8.7	1.8
	CSW	17	7.1	2.4	7	7.9	0.9
	MNE	22	6.4	3.5	18	4.8	3.8
	NCL	15	4.8	3.1	7	4.0	1.8
	BNC	13	9.5	1.4	8	7.9	1.0
	DSW	16	7.9	2.0	13	5.6	2.3
	TNE	11	8.7	1.3	10	8.7	1.1
5/2/79	TTS	18	15.4	1.1	8	17.0	0.5
	ELS	8	9.7	0.8	5	8.1	0.6
	YSW	16	9.7	1.6	6	14.6	0.4
	GMN	13	7.3	1.8	11	5.7	1.9
	ESW	6	4.1	1.5	6	6.5	0.9
	VWS	10	2.4	4.1	6	2.4	2.5

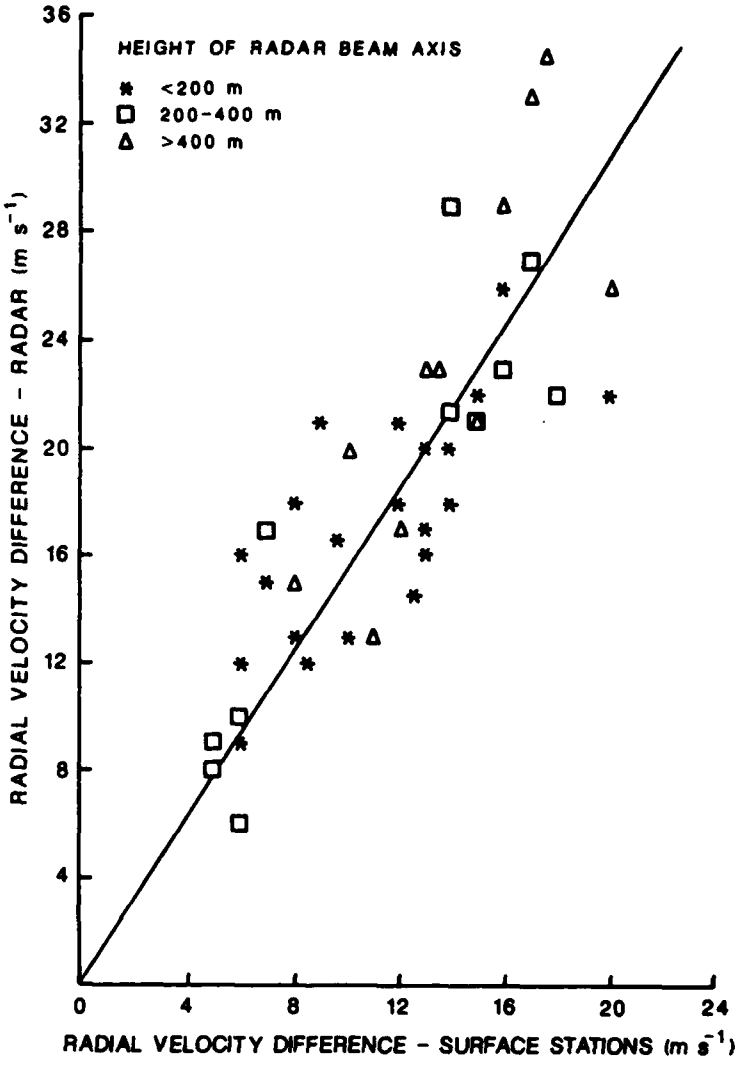

Figure 16. Velocity difference across gust front as measured by Doppler radar versus velocity difference measured at the surface by SAM stations. The code shows the approximate height of the Doppler radar observation. Notice that there is little difference in scatter about the line for the different height groups.

By examination of vertical wind profiles as measured by instruments on the tower during gust front passage we can determine why the radar-detected radial shear is stronger than that observed on the ground. Figures 17-21 are plots of radial velocity difference versus height across the five gust fronts as they passed the tower. The peak radial velocity behind the gust front is also shown in Figs. 17-19 to show how winds increase with height at low alti-

tudes and also to allow comparison with the radar in Fig. 17 because the leading edge of the gust front could not be delineated due to ground clutter. In two of the cases (May 2, 1979 and April 26, 1984) it was possible to directly compare radial velocities from the radar with that from the tower. The 2 May 1979 (Fig. 17) gust front profile illustrates why Doppler radar detects stronger radial velocities (and shear) at heights above the surface compared with surface measured velocities. In this case, the radar beam is pointed at a height of 220 m with vertical resolution of 430 m. This closely approximates the vertical extent of the tower. The peak velocity in the gust front measured by Doppler radar was 1.6 times the peak radial velocity measured at the lowest height of the tower (7 m). In the other case (April 26, 1984) where comparison between the tower and Doppler radar was possible (Fig. 20), the radar-estimated velocity difference is significantly larger than that observed at the 7 m height, this time by a factor of 1.4.

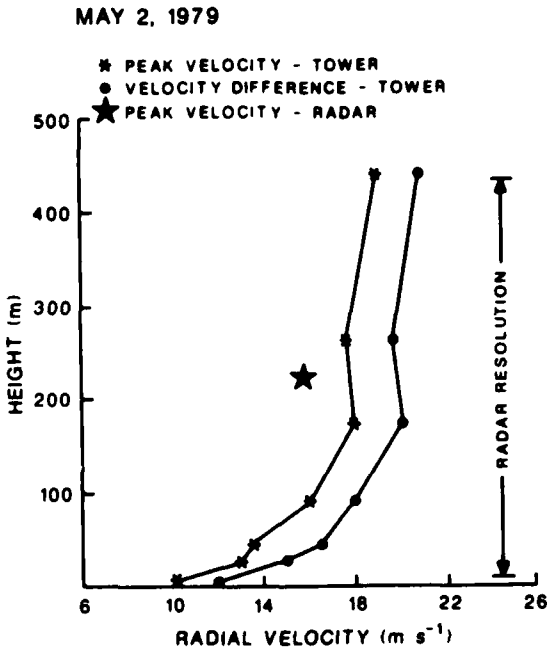

Figure 17. May 2, 1979 plot of radial velocity from the tower versus height showing increase in velocity and velocity difference with height. Also shown is the radar peak velocity at the same time.

Figure 18 is a plot of radial velocity (towards the Cimarron radar) difference and peak radial velocity as measured by instruments on the tower for the gust front of 6 June 1979. It is evident from this figure that all winds within gust fronts do not follow the logarithmic profile, however, strongest winds, and shear, are still removed from the surface by some distance (in this case ~90 m) due to frictional forces.

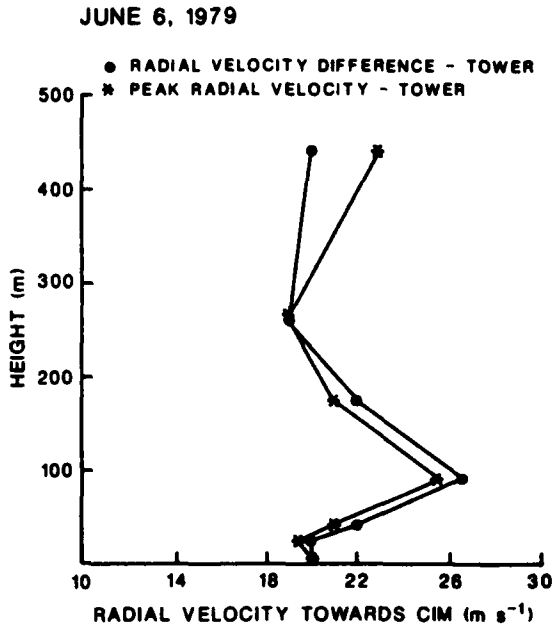

Figure 18. Same as Figure 17 except for June 6, 1979, although no radar data were available.

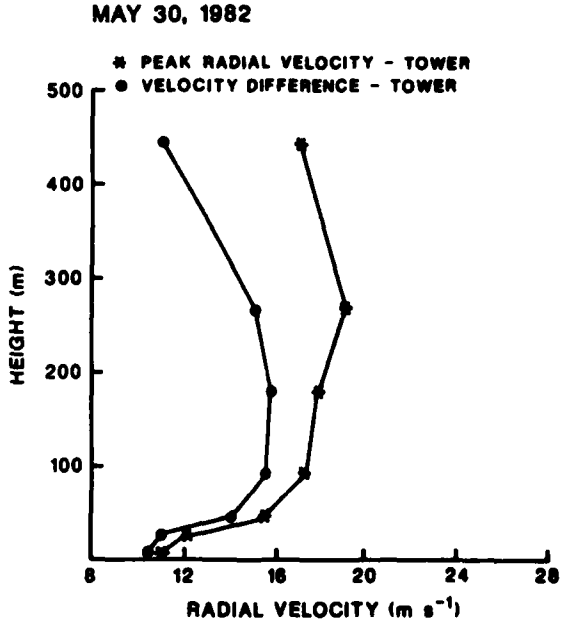

Figure 19. Same as Figure 18 except for May 30, 1982.

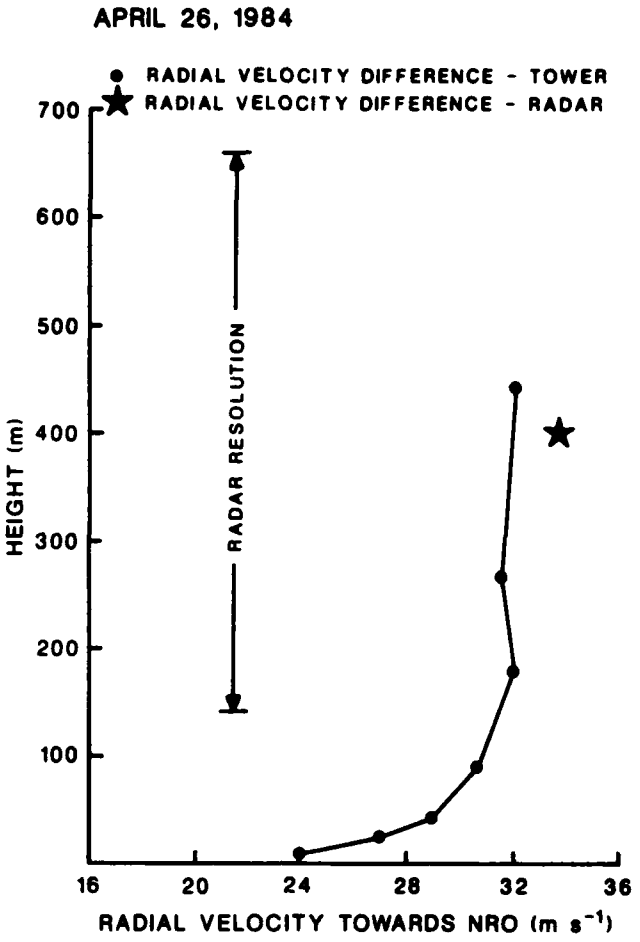

Figure 20. Same as Figure 17 except for April 26, 1984.

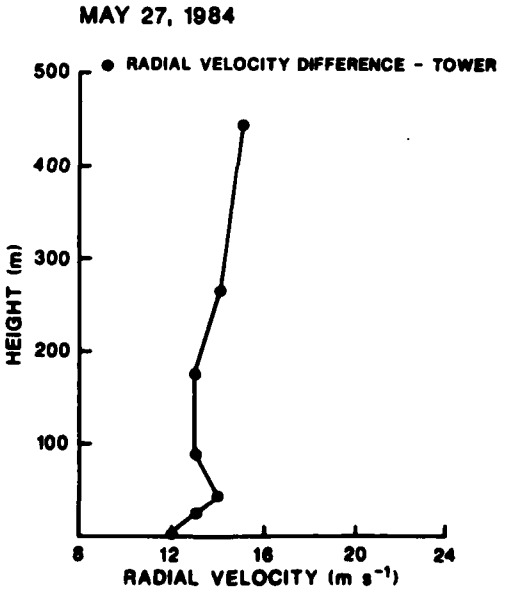

Figure 21. Same as Figure 18 except for May 27, 1984.

Figure 22 is a time history of the u-component (east-west, which is approximately perpendicular to the gust front) of the wind as the gust front of 2 May 1979 passed the tower. Because the vertical profiles of u are all 3 min apart, the horizontal separation between each pair of successive profiles is proportional to the shear that an aircraft would encounter when flying east-west through this gust front. Although this type of shear (convergent) may not in itself be dangerous to aircraft, it is obvious that the strongest shears are at least 90 m above the surface. Similar to Fig. 22, Fig. 23 gives profiles (1 min apart) for times after the gust front passage (divergent shear). Note that because profiles are spaced 1 min apart in Fig. 23, whereas they are spaced 3 min in Fig. 22, the divergent shear, which appears weaker than the convergent shear, is actually nearly as strong as the strongest convergent shear. The divergent shear profile, again, has the strongest shears removed from the surface by at least 90 m. This divergent shear is especially dangerous to aircraft because of its proximity to the gust front and its strong divergence. When an aircraft penetrates a gust front from either direction it instantly gains air speed and/or altitude. If the gust front were encountered during landing, the pilot would, after leaving the gust front, have to put the nose down and reduce thrust to land at the intended target. If he then encountered the divergent shear shown in Fig. 23, the situation would be dangerous. This divergent shear [16 m s^{-1} (2.8 km)$^{-1}$] behind the gust front (Fig. 23) is comparable with the average shear observed in the JAWS microbursts [24 m s^{-1} (3.1 km)$^{-1}$].

Thus we can see from Figs. 17-23 that for typical Oklahoma gust fronts we can expect the strongest shears to be at least 90 m above the surface. In Fig. 18 (the gust front of 6 June 1979) there is a peak in the shear at the 90 m level; hence it is possible to have peaks in the shear at low altitudes although these peaks will be removed from the surface because of frictional forces.

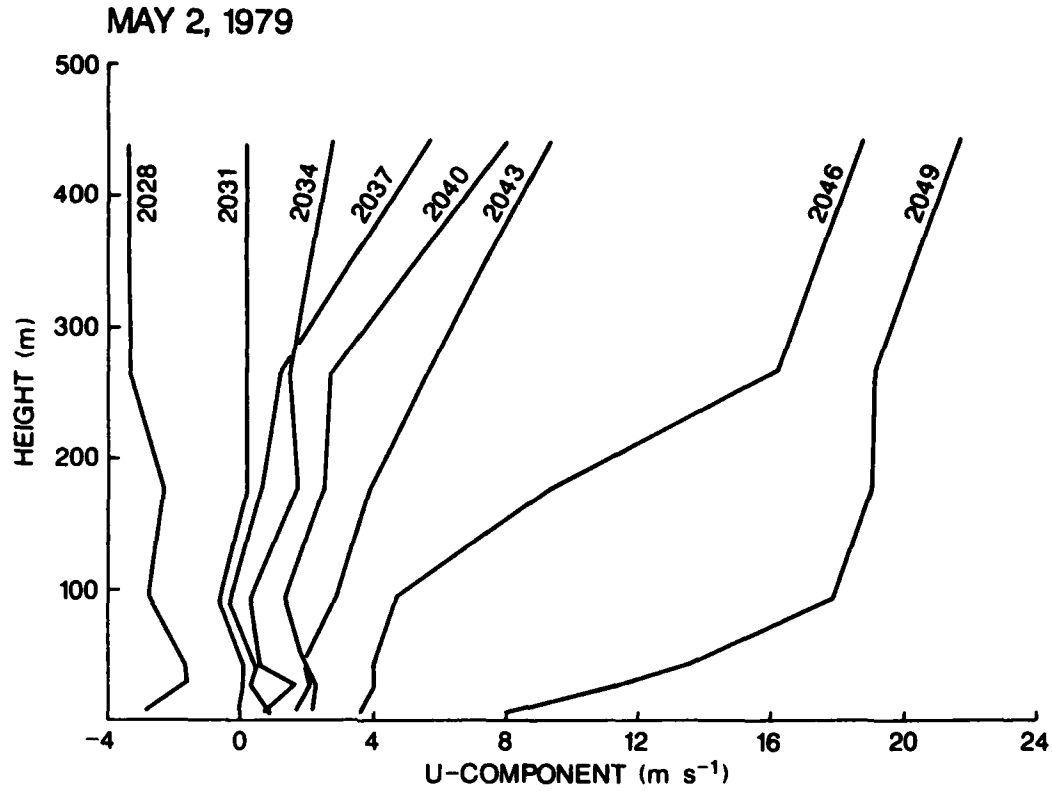

Figure 22. Plot of May 2, 1979 time history of u-component (east-west) of the wind during gust front passage.

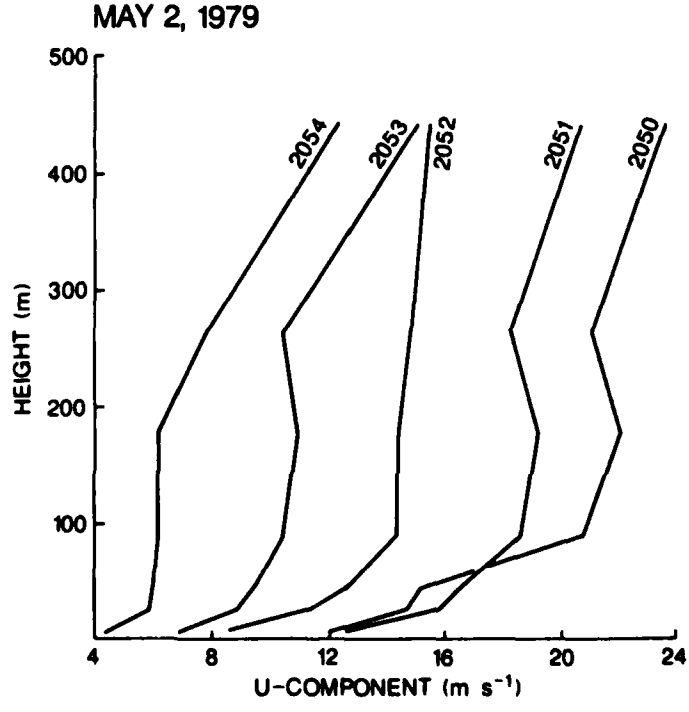

Figure 23. Same as Figure 22 except for times after gust front passage. Shear evident in this figure is divergent and is dangerous to aircraft encountering it.

7. Discussion and conclusions

Results from this study indicate that Doppler-radar-estimated shears measured at heights of 50-600 m in Oklahoma gust fronts are stronger than shears measured at the surface, by an average ratio of 1.6:1. Because of surface frictional forces, winds in the lowest 90 m are weaker than winds aloft, as are horizontal shears. Tower wind profiles measured during gust frontal passage (Figs. 17-23) confirm that winds near the surface (and shears) are weaker than winds (and shears) aloft. This is also confirmed by plots of gust front velocities with height shown by Klingle (1985), Goff et al. (1977), and others. Kessinger et al., (1983) have also shown that winds associated with a microburst are stronger aloft than at the surface. Thus, it is expected that frictional forces will slow winds near the surface for all conditions; thus, strongest winds and strongest shears will occur some distance above the surface. This distance will differ from environment to environment and from phenomenon to phenomenon. Furthermore, the presence of a surface-based inversion may cause surface flow fields and shears to be reduced even more than that due to just surface friction (Bedard, 1984).

The FAA requirements for Doppler radar coverage in the airport area call for the lowest scan to be less than 60 m above ground level at all points within 20 km of the airport. If this requirement is met, Doppler radar should be able to detect the maximum shears found in the airport area, especially shears found in the Oklahoma gust front environment. However, it is probably more important to determine whether Doppler radar can reliably estimate shear along a 3° glide slope that an aircraft will actually fly during departure or arrival. We can determine that in some cases a Doppler radar with vertical resolution of 365 m (the maximum allowed in the airport area) may underestimate the shear at the 90 m level of the tower, owing to the vertical resolu-

tion of the Doppler radar. For example, in Fig. 18 (which has a shear profile most susceptible to underestimation), a radar pointed at the 90 m height with resolution of 365 m (about the same resolution as a radar with 1° beam width at 20 km range) would in effect be averaging in the vertical over the lowest 273 m of the atmosphere. In this case a Doppler radar would underestimate the velocity difference across the gust front at the 90 m height by ~4 m s^{-1} (assuming uniform weighting in the vertical), which is 15% of the total velocity difference. Although there is some error in this shear estimate, it is still quite accurate. The viewing angle dependence of Doppler radar is thought likely to cause much more significant errors in estimates of shear than will the change of shear with height.

The determination that shears are stronger aloft than at the surface can be used to improve wind shear detection in the area surrounding airports, where wind shear is most hazardous to aircraft. Shears detected by a ground-based sensing device such as the Low-Level Wind Shear Alert System (LLWSAS) (Goff, 1980) will underestimate shears aloft. However, if estimates of shear at the surface were "corrected" with a factor of, say, 1.6 (which was found in this study to be the average ratio of shears aloft to shears at the surface), then they would be more comparable with the shears aloft where aircraft are actually flying.

Using a remote sensing system such as Doppler radar to detect shears aloft in the terminal area of an airport would be better than using surface stations to determine the actual shear along a flight path. However, this is true only if the Doppler radar is looking approximately along the flight path. One of the main problems with using Doppler radar to detect wind shears is the viewing-angle dependence of wind shear estimates.

If a combination of Doppler radar and surface data were used, the Doppler radar data to detect radial shear aloft and the surface data to determine which direction the strongest shear is, then a good estimate of the shear along a flight path would be possible.

Further study with Doppler radar, surface networks, and especially tall instrumented towers is needed to determine if a combination of Doppler radar and surface data will be able to reliably estimate shear along a flight path. Such studies should also determine at which height shears are strongest in different environments, and in different phenomena dangerous to aircraft (e.g., gust fronts, downbursts). Further knowledge gained from these studies will allow more accurate estimates by both Doppler radar and LLWSAS of wind shear hazardous to aircraft in the airport terminal area.

REFERENCES

Bedard, A.J., F.N. Merrem, D. Simms, and M.M. Cairns, 1979: A thunderstorm gust-front detection system. FAA Rep. FAA-RD-79-55, 130 pp.

Bedard, A.J., 1984, 1984: Optimizing the use of surface sensors for wind shear detection. J. Aircraft, 21(12), 971-977.

Businger, J.A., J.C. Wyngaard, Y. Izumi, and E.F. Bradley, 1971: Flux profile relationships in the atmospheric surface layer. J. Atmos. Science, 28, 181-189.

Clarke, R.H., 1970: Observational studies in the atmospheric boundary layer. Q. J. Roy. Meteor. Soc., 96, 91-114.

Cressman, G.P., 1959: An operational objective analysis system. Mon. Wea. Rev., 10, 367-374.

Doviak, R.J., and D.S. Zrnic', 1984: Doppler Radar and Weather Observations. Academic Press, Orlando, Florida, 458 pp.

Eilts, M.D., 1983: The structure of the convective boundary layer as seen by lidar and Doppler radars. Master's thesis, University of Oklahoma, 97 pp.

Eilts, M.D., and R.J. Doviak, 1986: Oklahoma downbursts and their asymmetry. J. Clim. Appl. Meteor., in print.

Eilts, M.D., and R.J. Doviak, 1987: Oklahoma downbursts and their asymmetry. FAA Final Report, in print, 56 pp.

FAA (Federal Aviation Administration), 1981: Terminal area weather radar detection and convective prediction development. Interagency Agreement DTFA01-81-Y-10521 between DOT/FAA and DOC/NOAA, Jan. 7, 1981.

Gandin, L.S., 1965: Objective analysis of meteorological fields. National Technical Information Service, U.S. Dept. of Commerce, Springfield, Virginia 22151, Order No. TT-65-50007, 242 pp.

Goff, R.C., J.T. Lee, and E.A. Brandes, 1977: Gust front analytical study. FAA Rep. FAA-RD-77-119, 126 pp.

Goff, R.C. 1980: The Low-Level Wind Shear Alert System (LLWSAS). FAA-RO-80-45, 120 pp.

Hjelmfelt, M.R., 1984: Radar and surface data analysis of a microburst in JAWS. Preprints, 22nd Conference on Radar Meteorology, Zurich, Switzerland, 10-14 Sept. AMS, Boston, Massachusetts, 58-63.

Kaimal, J.C., J.C. Wyngaard, D.A. Haugen, O.R. Cote, Y. Izumi, S.J. Caughey, and C.J. Readings, 1976: Turbulence structure in the convective boundary layer. J. Atmos. Sci., 33, 2152-2168.

Kessinger, C., M.R. Hjelmfelt, and J. Wilson, 1983: Low-level microburst wind structure using Doppler radar and PAM data. Preprints, 21st Conference on Radar Meteorology, Edmonton, Alberta, Canada, 19-23 Sept., AMS, Boston, Massachusetts, 609-615.

Klingle, D.L., 1985: A gust front case studies handbook. FAA Rep. FAA-PM-84/15, 108 pp.

Mahapatra, P.R., D.S. Zrnic', and R.J. Doviak, 1983: Optimum siting of NEXRAD to detect hazardous weather at airports. J. Aircr., 20(4), 363-371.

Mahapatra, P.R., and J.T. Lee, 1984: The role of NEXRAD in aircraft navigation and flight safety enhancement. J. Inst. Navig., 31(1), 21-37.

National Research Council, 1983: Low-altitude wind shear and its hazard to aviation. National Academy Press, Washington, D.C., 112 pp.

Wakimoto, R.M., 1982: The life cycle of thunderstorm gust fronts as viewed with Doppler radar and rawinsonde data. Mon. Wea. Rev., 110, 1060-1082.

Wilson, J.W., R.D. Roberts, C. Kessinger, and J. McCarthy, 1984: Microburst wind structure and evaluation of Doppler radar for airport wind shear detection. J. Clim. Appl. Meteor., 23, 898-915.

Zrnic', D.S., and J.T. Lee, 1983: Investigation of the detectability and lifetime of gust fronts and other weather hazards to aviation. FAA Rep. DOT/FAA/PM-83/33, 50 pp.